BUTTERWORTH HEINEMANN

Polymer Vol. 36 No. 4, pp. 837–842, 1995

0032-3861/95/$10.00+0.00

A novel method to fabricate bioabsorbable scaffolds

K. Whang, C. H. Thomas and K. E. Healy*
Department of Biological Materials, Northwestern University Dental School, 311 E. Chicago Avenue, Ward Building 10-019, Chicago, IL 60611-3008, USA, and Department of Biomedical Engineering, McCormick School of Engineering, Northwestern University, Evanston, IL, USA

and G. Nuber
Department of Orthopedic Surgery, Northwestern University Medical School, Chicago, IL, USA
(Received 30 June 1994; revised 8 August 1994)

An emulsion freeze-drying method for processing porous biodegradable copolymers of polylactic and polyglycolic acid (PLGA) scaffolds was developed. Scaffold porosity and pore sizes were measured using mercury porosimetry. Foams with porosity in the range 91–95%, median pore diameters ranging from 13 to 35 μm (with larger pore diameters greater than 200 μm), and specific pore area in the range 58–102 $m^2 g^{-1}$ were made by varying processing parameters such as water volume fraction, polymer weight percentage and polymer molecular weight. These scaffolds may find applications as structures that facilitate either tissue regeneration or repair during reconstructive operations.

(Keywords: tissue engineering; bioabsorbable polymers; emulsion processing)

INTRODUCTION

Materials that serve as analogues for the native extracellular matrix (ECM) can be used in medicine and dentistry to aid in either the reconstruction or regeneration of damaged tissue and organs. Polymer matrices have been used for regeneration of bone, cartilage, liver, skin and other tissues[1–10]. Polylactic acid (PLA), polyglycolic acid (PGA) and their copolymers (PLGA) are attractive materials for ECM analogues because they degrade by random hydrolysis when implanted, and their degradation products are ultimately expelled from the body as carbon dioxide and water[11]. An ideal matrix should have sufficient porosity for diffusion of nutrients and clearance of wastes, and have adequate mechanical stability to support and transfer loads. Other important factors in determining successful regeneration of tissue and organs are material surface chemistry, porosity, micro- and macrostructure of the pores, and shape of the scaffolds[6,8,12]. The surface chemistry of the material must allow cell adhesion and active cell-substratum events so that the cells express their normal phenotype[13]. Furthermore, the porosity, pore sizes, and the interconnections between the pores of the substrate affect tissue ingrowth into implants[7,12]. The effect of implant pore size on tissue regeneration is emphasized by experiments demonstrating optimum pore sizes of 20 μm for fibroblast ingrowth[15], between 20 and 125 μm for regeneration of adult mammalian skin[10] and 100–250 μm for regeneration of bone[15,16]. Thus, a major goal in fabricating scaffolds for tissue regeneration is the accurate control of pore size and porosity.

Macroporous, biodegradable polymer scaffolds have been prepared by numerous techniques including solvent casting/salt leaching[3,6], phase separation[17], solvent evaporation[18], and fibre bonding to form a polymer mesh[3,7]. Solvent casting/salt leaching involves mixing solid impurities, such as sieved sodium chloride particles, into a polymer solvent solution, and casting the dispersion to produce a membrane of polymer and salt particles. The salt particles are then leached out with water to yield a porous membrane. Porosity (87–91%) and pore size (100–500 μm in diameter) have been shown to be dependent on salt weight fraction and particle size[3,6]. Phase separation involves dissolving a polymer in a suitable solvent, placing it in a mould, then cooling the mould rapidly until the solvent is frozen. The solvent is removed by freeze-drying, leaving behind the polymer as a foam with pore sizes of 1–20 μm in diameter[17].

An initial goal of this research programme was to develop a novel processing technique to fabricate highly porous implantable PLGA scaffolds, with the restriction that the technique must ultimately be amenable to eventual incorporation of protein-based growth and differentiation factors for subsequent controlled delivery. More specifically, this involves fabricating scaffolds with porosity greater than 90% and the ability to control pore sizes ranging between 20 and 200 μm. The aforementioned methods are unsuitable owing to either the inability to incorporate protein-based growth factors (solvent casting/salt leaching, polymer mesh) or the

* To whom correspondence should be addressed at the first address given

inability to form large pores, i.e. 50–200 μm (phase separation, solvent evaporation). This paper addresses a novel method of fabricating bioabsorbable scaffolds with variable porosity and pore sizes. Quantitative evaluation of fabrication parameters that control porosity, pore sizes and characterization of the physical properties of these materials is the subject of another report.

The method proposed in this work consists of creating an emulsion by homogenization of a polymer solvent solution and water, rapidly cooling the emulsion to lock in the liquid-state structure, and removing the solvent and water by freeze-drying. Thus, knowledge of the theory of emulsions allows processing variables to be identified that affect the liquid-state structure of the emulsion and hence the macro- and microporous structure of the solid scaffolds. However, not all the assumptions hold firmly, so the following theories are only applicable in guiding choices of processing parameters to be investigated.

To create an emulsion from two immiscible phases, where the continuous phase contains the polymer-rich solvent and the dispersed phase is water, the control of various processing factors is very important, e.g. volume fraction of the dispersed phase, ϕ. Furthermore, the effect of emulsion stability on scaffold pore structure also has to be considered since emulsions are usually not thermodynamically stable systems and artifacts like creaming, flocculation and coalescence can be introduced which cause poorly dispersed pores. Physical properties and forces involved in emulsion stability include the interfacial free energy[19], the relative viscosity increment[20], gravity[21], the diffusion coefficient of the dispersed particles, the height of the free-energy barrier preventing coagulation[22] and the electrical repulsive force between particles as defined via the Deryagin Landau Verwey Overbeek (DLVO) theory[22].

It is clear that emulsions present a large interfacial area, and any reduction in interfacial free energy will reduce the driving force towards coalescence, promoting stability. The presence of an emulsifier should reduce the interfacial free energy and thereby stabilize the emulsion[19]. In this work, the polymer acts as an emulsifier even though it was not specifically chosen for that purpose. By varying the polymer wt% and $\overline{M}_w$ (weight-average molecular weight), the effectiveness of this polumer as an emulsifier and hence the stability of the emulsion can be affected, that is, by increasing the polymer wt% and $\overline{M}_w$ the stability of the emulsion should increase.

The relative viscosity increment, η_i, may be an important factor in emulsion stability when shear stress is applied during homogenization, since it affects the relative motion and interaction of the dispersed colloidal particles. (The relative viscosity increment is analogous to the specific viscosity, but the use of the latter term is discouraged by the IUPAC[20].) The relative viscosity increment is described by Einstein's expression for specific viscosity of rigid spheres in a solvent system[20].

$$\eta_i = 2.5\phi + 6.2\phi^2 + k_3\phi^3 + \ldots \quad (1)$$

where k_3 is a constant determined empirically[20]. Although this equation was originally derived for colloidal suspensions, it may be applicable as a qualitative guide for identifying processing parameters in emulsion systems that contain emulsifiers. The system used in this paper contains a polymer in solution which acts as an emulsifier, hence this equation may be used in identifying ϕ as a processing parameter that affects the emulsion structure and stability. In this equation, η_i is shown to be directly related to ϕ since increasing ϕ allows larger aggregates and increases η_i[20]. Thus η_i affects the ease with which dispersed particles will interact with each other[20] and may also be related to the viscosity of the emulsion, which in turn affects emulsion stability[21].

The stability of emulsions is also affected by the rate of creaming due to gravitational effects on the difference in density of the dispersed and continuous phases. This rate of creaming in the emulsion is approximated by Stoke's Law (equation (2))[21]:

$$\frac{dx}{dt} = \frac{2r^2(\rho_d - \rho_c)g}{9\eta} \quad (2)$$

where x is an arbitrary coordinate system, g is the gravitational constant, r is the radius of the dispersed phase particle and η the viscosity of the emulsion. This equation was originally derived with the assumption that the dispersed phase consists of rigid, spherical, non-interacting particles, which is not the case for systems addressed in this paper, so equation (2) can only be used as a guide to select parameters that may help stabilize the emulsion[21]. In equation (2), the terminal velocity of a particle (dispersed phase), dx/dt, determined by the gravitational force on the dispersed phase with density ρ_d (water) and resisted by the viscous force of the continuous phase with density ρ_c (polymer solution), is the rate at which creaming may take place due to gravitational effects. This rate is directly proportional to the difference in densities between the two phases and inversely proportional to the viscosity of the emulsion[21]. Thus r, ρ_d, ρ_c and η should influence the stability of the emulsion via gravitational effects and hence the macroporous structure[21]. In this work, r is not a controllable parameter and ρ_d is fixed, but ρ_c and η can be varied by varying polymer wt%, ϕ and polymer $\overline{M}_w$. Note that as $\overline{M}_w$ increases the viscosity of the polymer solution increases due to an increase in inherent viscosity, η_{inh}[23,24].

Emulsion stability is also affected by the rate of flocculation and coalescence, determined by three components: the height of the free-energy barrier preventing coagulation (V_{max}), the electrical repulsive force between particles[22] and the diffusion coefficient of the dispersed particles[19]. These components are summarized in equation (3), which was modified by Everett[22] from the original work by Smoluchowski (1918) and Müller (1926), to describe the inhibition of coagulation of particles due to the height of the free-energy barrier and the electrical repulsive force between particles (equation (5))[22]. Assuming that the dispersed particles in this work are spheres, the Stokes–Einstein expression for the diffusion coefficient can be used (equation (4))[19].

$$\frac{dv}{dt} = -8\pi R D v^2 W \quad (3)$$

$$D = \frac{kT}{3\pi\eta_c R} \quad (4)$$

$$W = \frac{1}{\kappa R}\exp\left(\frac{V_{max}}{kT}\right) \quad (5)$$

Here v is the concentration of single particles (i.e. in

dispersed phase), dv/dt is the rate at which they disappear, R is the diameter of the particles, D is the Stokes–Einstein expression for the diffusion coefficient for spheres, k is Boltzmann's constant, T is absolute temperature, η_c is the viscosity of the continuous phase (note that this nomenclature is not in the reference cited but is used here to reduce any confusion between the viscosities of the emulsion and the continuous phase), W is a parameter describing the decrease in the coagulation rate, $1/\kappa$ is the Debye length, and V_{max} is the height of the free-energy barrier preventing coagulation[22]. Equations (3)–(5) show that the rate of flocculation and coagulation is inversely proportional to the viscosity of the continuous phase, V_{max}, and the electrical repulsive force between two charged dispersed particles approximated by κR[22]. The choice of polymer, which acts as an emulsifier, and the dispersed phase material may affect V_{max} and κR, but these are set parameters in the method presented here. However, η_c, V_{max} and κR can be varied by varying polymer wt% and polymer $\overline{M}_w$. Increasing polymer wt% and $\overline{M}_w$ should increase η_c. An increase in $\overline{M}_w$ also increases κR and V_{max} since the longer chain of the emulsifier increases the thickness of the double layer between two particles in suspension[22]. These effects can be used to reduce the rate of flocculation.

In short, the emulsion structure can be stabilized by altering polymer wt%, $\overline{M}_w$ and ϕ, to control η_i, ρ_c, η, V_{max}, κR and η_c, thus altering the interaction of the dispersed particles and allowing sufficient time to freeze the emulsion and lock in the macroporous structure prior to extensive creaming, flocculation or coagulation of the dispersed phase.

MATERIALS AND METHODS

Materials

DL-lactide/glycolide copolymers of 85:15 (lactide glycolide) mole ratio, and η_{inh} of 0.25, 0.51 and 0.79 dl g^{-1} were obtained from Birmingham Polymers Inc. (Birmingham, AL). Methylene chloride (MC) was obtained from Baxter Diagnostics Inc. (McGraw Park, IL) and was used as received.

Fabrication of scaffolds

A schematic diagram of the fabrication process is shown in *Figure 1*. The polymer was first dissolved in MC such that it would have the desired wt% to the total volume (5 ml) of emulsion. Appropriate volumes of the polymer–MC solution and ultrapure water (ASTM grade 1, 18 Mohm) were added together in a glass test-tube so that the desired value of ϕ was achieved. The η_{inh} and ϕ values of the polymer and polymer wt% used in each sample are listed in *Table 1*. The immiscible layers were homogenized, using a handheld homogenizer (Omni Int., Waterbury, CT), then poured into a cylindrical copper mould (internal diameter = 2.54 cm; height = 3 cm), and quenched by quickly placing the mould into a copper container that was maintained near liquid nitrogen temperature (~ −196°C). When all the samples were quenched, they were freeze-dried (Virtis Co. Inc., Gardiner, NY) at a pressure of 30 mTorr and temperature of −55°C. Samples were placed in a vacuum desiccator at room temperature for at least 7 days to remove any residual solvent.

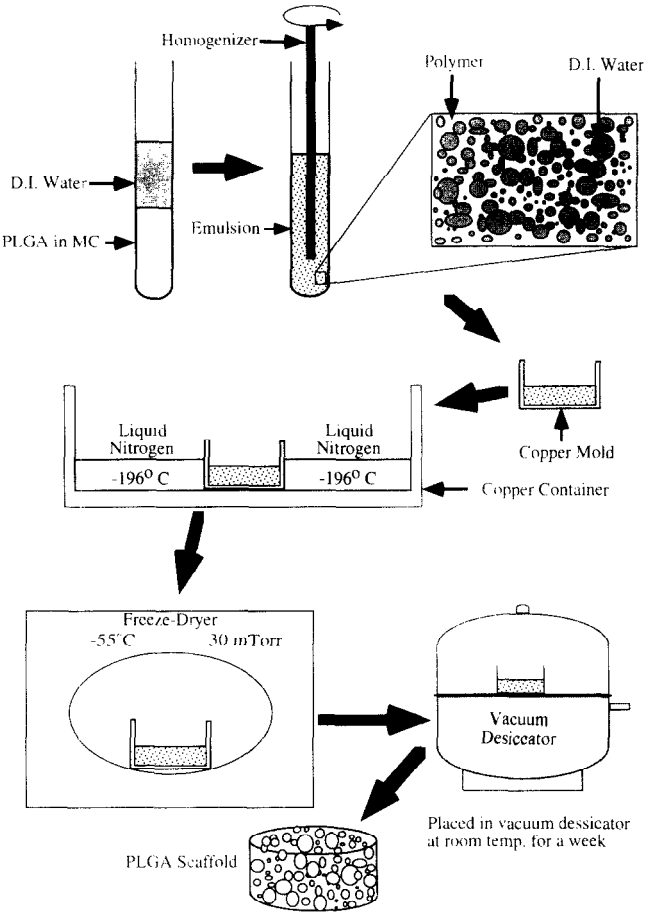

Figure 1 Schematic representation of the emulsion freeze-drying method to fabricate PLGA scaffolds. The polymer was dissolved in MC, to which ultrapure water was added, forming two immiscible layers. These layers were homogenized to form an emulsion with water as the dispersed phase and the polymer solvent as the continuous phase (water-in-oil). The emulsion was poured into a copper mould and quenched by placing into a copper container that was maintained near liquid nitrogen temperature (~ −196°C). Once frozen, the samples were freeze-dried

Table 1 Processing variables for scaffolds

Sample	η_{inh} (dl g^{-1})	ϕ	Polymer (wt%)
1	0.79	0.4	10.0
2	0.51	0.5	7.5
3	0.51	0.4	7.5

Scanning electron microscopy (SEM) analysis

After a week in the vacuum desiccator, the samples were cut in half using a sharp razor blade, a thin piece was sheared from the centre, sputtered with gold (SCD 040 sputtering machine, Balzers, CT), and observed using SEM.

Mercury porosimetry analysis

Samples were analysed by mercury porosimetry using an AutoPore II 9220 (Micromeritics, Norcross, VA) to determine pore size distributions, specific pore area, median pore diameter and porosity. A solid penetrometer volume ranging from 6.7 to 7.3 ml and samples weighing about 0.1 g were used. Mercury was filled from a filling pressure of 3.4 kPa (0.5 psia) and intruded to a maximum

pressure of 414 MPa (60 000 psia). The relationship between the filling pressure and pore radius is given by the Washburn equation[25]:

$$r = -2\gamma \cos(\theta)/P \quad (4)$$

where γ is the surface tension of mercury (~ 480 dyne cm^{-1}) and θ is the contact angle between mercury and the polymer surface[26]. Equation (4) gives the corresponding radius of a cylindrical pore[27]. The sessile drop contact angle between mercury and the solvent-cast PLGA film was measured with a customized micrometer microscope fitted with a goniometer eyepiece (Gaertner, Chicago, IL) at ambient temperature[28]. The three-phase contact angle between the liquid (mercury), vapour and the surface (polymer) was $137 \pm 1°$ ($n = 4$), and was used to calculate the pore diameter from the intrusion pressure.

RESULTS

SEM analysis

Scanning electron micrographs of three different scaffolds are shown in *Figures 2a–c*. Even though there is a large distribution in pore size for a given sample, clear differences in the average pore size are evident, with sample 1 having the largest pores and sample 3 having the smallest. All samples were highly porous with good interconnections between pores, and they were physically stable and manageable.

Mercury porosimetry analysis

Mercury porosimetry analysis demonstrates the ability of the fabrication technique to create scaffolds with high porosity and varying pore size. These samples gave average porosities ranging from 91 to 95%, median pore sizes ranging from 15 to 35 μm, and specific pore areas ranging from 58 to 102 $m^2 g^{-1}$ (*Table 2*). However, the largest pores were greater than 200 μm in all the samples, as is evident in *Figure 3*, which shows the plots of the log differential intrusion *versus* pore diameter of the scaffolds. This distribution of pore sizes was also depicted in the SEM micrographs in *Figure 2*. There is also a clear distinction of two types of pores: those larger than about 1 μm and those much smaller, < 0.01 μm. The pores larger than 1 μm are mostly due to the emulsion while the much smaller pores are probably due to the inherent porosity of the polymer itself from the evaporation of the solvent, similar to those found in phase-separated foams. The porosimetry and SEM results verify the influence that varying processing variables have on scaffold properties, i.e. porosity, pore size distribution and specific pore area.

These results must be examined within the context that there are artefacts in mercury porosimetry measurements that distort the data to give low values for pore size. First, samples are compressed from the high pressures used to make measurements. Second, to access a certain pore, the mercury may need to penetrate the surface through a series of smaller pores, in which case the volume of that larger pore will be accredited to pores with smaller diameters[26]. These artifacts are most pronounced when

Table 2 Mercury porosimetry results

Sample	Porosity (%)	Median pore size (μm)	Specific pore area ($m^2 g^{-1}$)
1	91	35	58
2	95	22	102
3	93	15	99

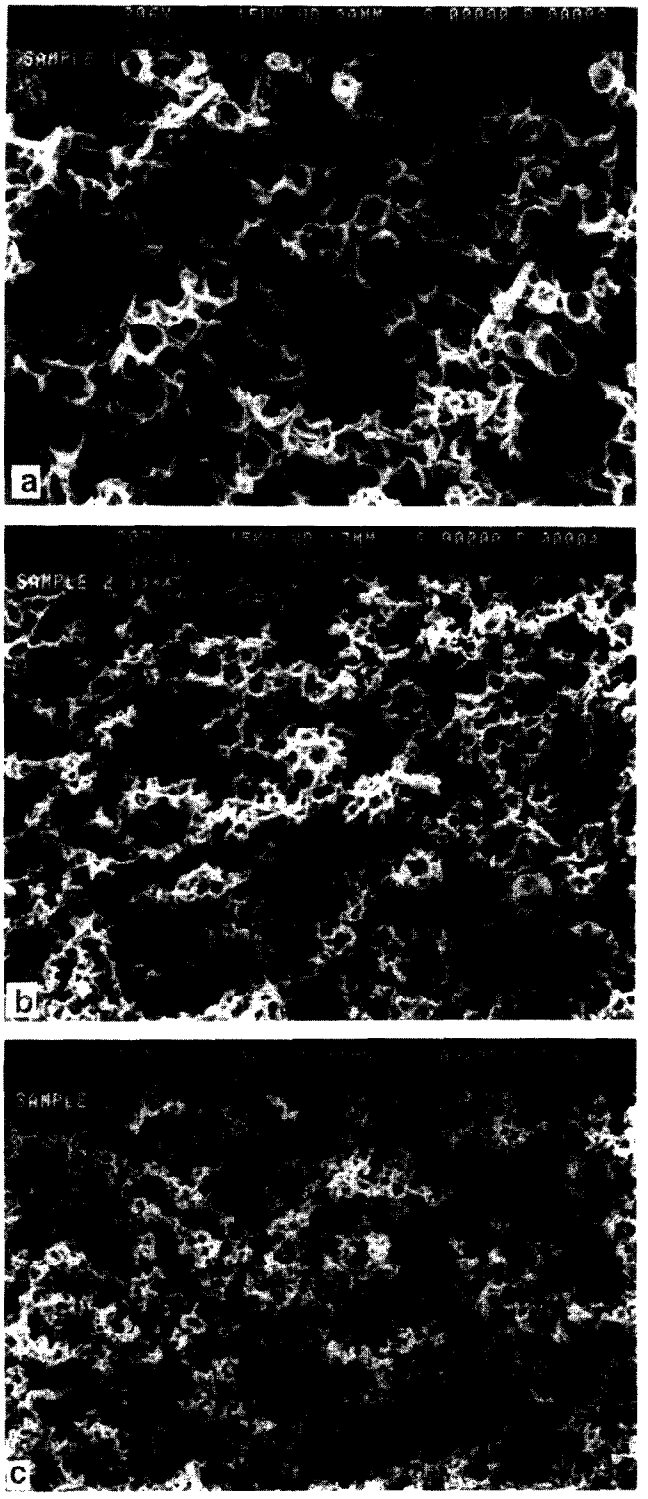

Figure 2 SEM micrographs of PLGA scaffolds made using the emulsion freeze-drying process. (a) Sample 1 has a porosity of 91%, median pore size of 35 μm and specific pore area of 58 $m^2 g^{-1}$. The processing variables are: $\eta_{inh} = 0.79$ dl g^{-1}, $\phi = 0.4$, and 10 wt%. (b) Sample 2 has a porosity of 95%, median pore size of 22 μm and specific pore area of 102 $m^2 g^{-1}$. The processing variables are: $\eta_{inh} = 0.51$ dl g^{-1}, $\phi = 0.5$, and 7.5 wt%. (c) Sample 3 has a porosity of 93%, median pore size of 15 μm and specific pore area of 99 $m^2 g^{-1}$. The processing variables are: $\eta_{inh} = 0.51$ dl g^{-1}, $\phi = 0.4$, and 7.5 wt%

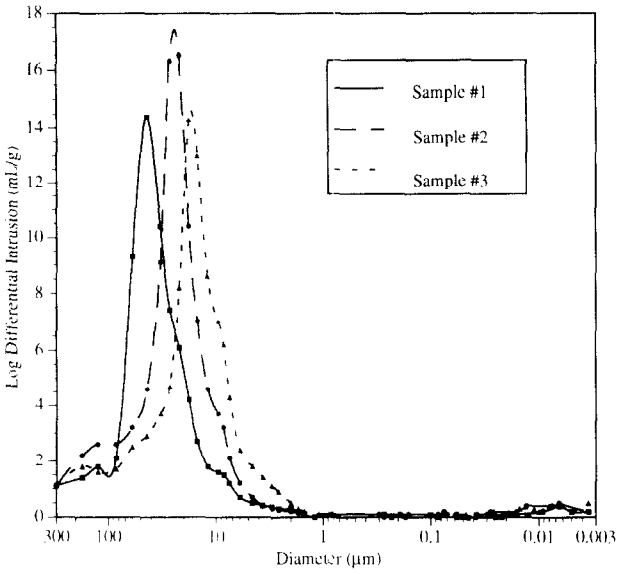

Figure 3 Pore size distributions. The ordinate represents the logarithm of the derivative of intrusion volume with respect to diameter, and the abscissa the diameter of the pore for that specific intrusion pressure as calculated using the Washburn equation assuming a sessile drop contact angle of 137°. Mercury was intruded from a filling pressure of 0.5 to 60 000 psia. The largest pores are greater than 200 μm in all three samples and a clear distinction of two types of pores was seen ($d > 1$ μm and $d < 0.1$ μm). A broad distribution of pores is also evident in this graph as well as three distinct peaks signifying differing median pore sizes

the pore size distribution is broad and from the SEM micrographs in *Figures 2a–c*, it is evident that there are many smaller pores that would create this type of artefact. For these reasons, the median pore sizes presented are lower estimates than the actual values and should be interpreted with the accuracy of the technique in mind.

DISCUSSION

A novel scaffold fabrication method was developed and it was shown that porosity, pore size and specific pore area can be varied by changing processing factors such as ϕ, polymer wt% and polymer η_{inh} (i.e. polymer $\overline{M_w}$). Emulsions have been used in industry to create porous foams, but the foams have been made by either polymerizing monomers in the emulsion, or extracting out the disperse phase using a wash/soak process and then drying[29]. These may be acceptable processes for non-health-care industries, but the use of crosslinkers such as divinylbenzene and surfactants are in most cases unacceptable for implantable devices. The emulsion freeze-drying process reduces most of the toxic chemicals and many of the processing steps cited above. Freeze-drying extracts the dispersed water and polymer solvents, eliminating the need for several wash/soak steps. Furthermore, the use of polymers instead of monomers alleviates the need for crosslinkers, and in this system surfactants (other than the polymer) are not necessary.

Qualitative comparison of the processing parameters in *Tables 1* and *2* shows that ϕ directly affects median pore size and indirectly affects porosity. Foams of good quality (i.e. porosity >80%) were not achieved when ϕ was less than 0.4. Sample 2 with $\eta_{inh} = 0.51$ dl g^{-1}, $\phi = 0.5$ and wt% = 7.5 gave the highest porosity and specific pore area. Sample 3 with $\eta_{inh} = 0.51$ dl g^{-1}, $\phi = 0.4$ and wt% = 7.5 gave the lowest median pore size. A decrease in ϕ from 0.5 to 0.4 decreased the median pore size from 22 to 15 μm, but kept the porosity, 95–93%, and the specific pore area, 102–99 m^2 g^{-1}, relatively constant. Examination of *Figure 3* clearly shows the difference in the distributions of mercury intrusion volume with respect to pore diameter for samples 2 and 3.

Median pore size also seems to be directly affected by the viscosity of the polymer solution, with sample 1 being most viscous due to a high η_{inh} and polymer wt%, having the greatest median pore size. This relationship may actually be more accurately described in terms of a relationship with polymer η_{inh}, because a higher $\overline{M_w}$ will give the emulsion structure more stability, allowing larger pores to be formed. In other words, an increase in $\overline{M_w}$ decreases the rate of creaming, according to equation (2), by increasing ρ_c and η, and decreases the rate of flocculation, according to equations (3)–(5), by increasing V_{max}, κR and η_c.

This technique was shown to be capable of producing scaffolds of PLGA with porosity greater than 90%, median pore sizes ranging from 15 to 35 μm in diameter with the largest pores greater than 200 μm, specific pore areas ranging from 58 to 102 m^2 g^{-1}, and good interconnections between the pores. These scaffolds have good physical properties and can be easily handled. The porosity and pore sizes are comparable to other materials used in cell transplantation and reconstructive surgery[3,6], but are somewhat smaller than those observed for fibre-bonded structures[7,9]. Though the median pore sizes appear small, it must be noted that the specific pore area is tremendously high, approximately two orders of magnitude greater than previously reported values[3]. This ability to control and produce such large specific pore areas may prove to be very important in the controlled delivery of drugs and tissue regeneration. The scaffolds made with this method are not membranes and can be made thick (>1 cm) compared with those made via a solvent casting/salt leaching method[27]. These scaffolds should prove useful in applications for tissue regeneration or reconstruction.

CONCLUSIONS

An emulsion freeze-drying technique was developed to fabricate PLGA polymer scaffolds with porosity, pore sizes and specific pore area depending on the processing parameters. Scaffolds with porosity greater than 90%, median pore sizes ranging from 15 to 35 μm with larger pores greater than 200 μm, and highly interconnected pores necessary for tissue ingrowth and regeneration were fabricated. Increases in ϕ and η_{inh} increased the median pore size.

ACKNOWLEDGEMENTS

This work was supported by a grant from the Department of Orthopedic Surgery at Northwestern University, to G.N. and K.E.H. The assistance of Peter Min during initial experiments is gratefully acknowledged.

REFERENCES

1 Gombotz, W., Bouchard, L., Pankey, S., Hawkins, M. and Poulakkainen, P. *Proc. Int. Symp. Control. Rel. Bioact. Mater.* 1993, **20**, 150

2 Cooper, M. L., Hansbrough, J. F., Spielvogel, R. L., Cohen, R., Bartel, R. L. and Naughton, G. *Biomaterials* 1991, **12**, 243
3 Freed, L. E., Marquis, J. C., Nohria, A., Emmanual, J., Mikos, A. G. and Langer, R. *J. Biomed. Mater. Res.* 1993, **27**, 11
4 Haberstadt, C., Anderson, P., Bartel, R., Cohen, R. and Naughton, G. *Mater. Res. Soc. Symp. Proc.* 1992, **252**, 323
5 Lucas, P. A., Laurencin, C., Syftestad, G. T., Domb, A., Goldberg, V. M., Caplan, A. I. and Langer, R. *J. Biomed. Mater. Res.* 1990, **24**, 901
6 Mikos, A. G., Wald, H. L., Sarakinos, G., Leite, S. M. and Langer, R. *Mater. Res. Soc. Symp. Proc.* 1992, **252**, 353
7 Mikos, A. G., Bao, Y., Cima, L. G., Ingber, D. E., Vacanti, J. P. and Langer, R. *J. Biomed. Mater. Res.* 1993, **27**, 183
8 Mooney, D. J., Cima, L. and Langer, R. *Mater. Res. Soc. Symp. Proc.* 1992, **252**, 345
9 Vacanti, C. A., Cima, L. G., Ratkowski, D., Upton, J. and Vacanti, J. P. *Mater. Res. Soc. Symp. Proc.* 1992, **252**, 367
10 Yannas, I. V., Lee, E., Orgill, D. P., Skrabut, E. M. and Murphy, G. F. *Proc. Natl Acad. Sci.* USA, 1989, **86**(3), 933
11 Cutright, D. E., Perez, D., Beasley, J. D., Larson, W. J. and Posey, W. R. *Oral Surg.* 1974, **37**, 142
12 Cima, L. G., Vacanti, J. P., Vacanti, C., Ingber, D., Mooney, D. and Langer, R. *J. Biomech. Eng.* 1991, **113**, 143
13 Healy, K. E., Tsai, D. and Kim, J. E. *Mater. Res. Soc. Symp. Proc.* 1992, **252**, 109
14 Sauer, B. W., Weinstein, A. M., Klawitter, J. J., Hulbert, S. F., Leonard, R. B. and Bagwell, J. G. *J. Biomed. Mater. Res.* 1974, **8**, 145
15 Klawitter, J. and Hulbert, S. *J. Biomed. Mater. Res. Symp.* 1983, **2**(1), 161
16 Spector, M., Michno, M. J., Smarook, W. H. and Kwiatkowski, G. T. *J. Biomed. Mater. Res.* 1978, **12**, 655
17 Aubert, J. H. and Clough, R. L. *Polymer* 1985, **26**, 2047
18 Gogolewski, S. and Pennings, A. J. *Makromol. Chem. Rapid Commun.* 1983, **4**, 675
19 Adamson, A. W. 'Physical Chemistry of Surfaces', John Wiley, New York, 1990, pp. 525–535
20 Everett, D. H. 'Basic Principles of Colloid Science', The Royal Society of Chemistry, London, 1989, pp. 115–120
21 Schramm, L. L. *Adv. Chem. Ser.* 1992, **231**, 1
22 Everett, D. H. 'Basic Principles of Colloid Science', The Royal Society of Chemistry, London, 1989, pp. 130–143
23 Rosen, S. L. 'Fundamental Principles of Polymeric Materials', John Wiley, New York, 1982, pp. 58–59
24 Young, R. J. and Lovell, P. A. 'Introduction to Polymers', Chapman and Hall, London, 1991, pp. 196–197
25 Ritter, H. L. and Drake, L. C. *Ind. Eng. Chem.* 1945, **17**, 782
26 Smith, D. M., Hua, D. W. and Earl, W. L. *MRS Bull.* 1994, **XIX**(4), 44
27 Mikos, A. G., Sarakinos, G., Leite, S. M., Vacanti, J. P. and Langer, R. *Biomaterials* 1993, **14**(5), 323
28 Healy, H. E., Lom, B. and Hockberger, P. E. *Biotechnol. Bioeng.* 1994, **43**, 792
29 Even, W. R. and Gregory, D. P. *MRS Bull.* 1994, **XIX**(4), 29